ELSEVIER

Journal of Crystal Growth 217 (2000) 360–365

GROWTH

www.elsevier.nl/locate/jcrysgro

Segregation of Ga in Ge and InSb in GaSb

P.S. Dutta, A.G. Ostrogorsky*

Department of Mechanical Engineering, Aeronautical Engineering and Mechanics, Rensselaer Polytechnic Institute, Troy, NY 12180, USA

Received 21 January 1999; accepted 20 April 2000
Communicated by R.S. Feigelson

Abstract

Axial and radial segregation of (i) Ga in Ge and (ii) InSb in GaSb has been evaluated in crystals grown by the submerged heater method. The values of diffusion coefficients obtained by fitting the Tiller's equation to the initial transients in composition are significantly lower than the values in the literature, obtained by using shear cells with capillaries.

PACS: 71.55.Eq; 81.10.Fq; 81.30.Fb; 64.75. + g

Keywords: Ge; GaInSb; Segregation; Submerged baffle; Diffusion coefficients

1. Introduction

Dopant and alloy segregation is a key phenomenon occurring during directional solidification of semiconductors. Segregation leads to non-uniform spatial electrical and optical properties and alloy composition in the wafers obtained from various sections of the crystal. The compositional homogeneity in the growing crystal is strongly affected by melt convection near the solid–liquid interface. Uniform distribution of impurities (having equilibrium segregation coefficient $k \neq 1$) is achieved only when all impurities, which are absorbed at the melt–crystal interface, are continuously replenished from the bulk melt. Steady replenishment can occur only if the growth rate R is constant, melt convection is steady and predictable, and the concentration of impurities in the bulk melt remains constant during growth [1]. These conditions are not satisfied during normal freezing on earth because of buoyancy-driven convection. Steady-state segregation was reported only in a few space-grown crystals [2]. More recently, directional solidification under terrestrial conditions by (a) application of magnetic fields during crystal growth [3–5] and (b) employing a submerged heater in the melt near the growth interface [6], the required conditions for steady-state growth by normal freezing and zone solidification techniques have been met. Strong reduction in convective interference with segregation was demonstrated by the latter technique in a large number of experiments with various materials system [7–9]. In particular, exceptionally uniform steady-state segregation was recently obtained in Te-doped GaSb by using large seeds in conjunction with an un-powered

* Corresponding author. Present address: Center for Microgravity and Materials Research, The University of Alabama in Huntsville, Huntsville, AL 34899, USA. Tel.: + 1-256-890-6944; fax: + 1-256-890-6050.

E-mail address: ostroga@email.uah.edu (A.G. Ostrogorsky).

0022-0248/00/$ - see front matter
PII: S0022-0248(00)00483-8

submerged heater (i.e. baffle) [10]. According to the analytical model and scaling analysis [11,12] this was possible because the equilibrium segregation coefficient of Te in GaSb, $k = 0.37$, is not much less than one, and because of the relatively low diffusion coefficient, $D = 1 \times 10^{-5}\,\mathrm{cm}^2/\mathrm{s}$.

The present work has been carried out with two key semiconductor model systems: Ga-doped Ge and dilute GaInSb alloy. Both systems have low equilibrium segregation coefficients ($k = 0.087$ and 0.1, respectively), which according to the models, makes steady-state growth a challenge. As in the previous work on Te-doped GaSb [10] we have employed single crystal seeds of the same diameter as the crystal, which simplifies the analysis of axial and radial segregation because of the absence of the cone region typical for vertical Bridgman growth. In the cone region, the area of the growing crystal changes continuously until the final diameter of the crystal is reached. As a result the shape of the melt–crystal interface changes due to constantly varying radial temperature gradient. This in turn induces de-stabilizing conditions at the growth interface and leads to convective interference [13]. As will be discussed, the analysis of the dopant profiles yields values of diffusion coefficients of Ga in Ge and InSb in GaSb which are lower than the accepted values in the literature, measured using shear cells with capillaries [14–17].

2. Experimental procedure

Synthesis of $Ga_{0.98}In_{0.02}Sb$ has been carried out in a multi-zone Mellen furnace [10] in 20 mm diameter flat bottom silica crucibles from 6N pure Ga, In and Sb without chemical treatment. The submerged baffle was used to mix the charge during synthesis [10]. The synthesized $Ga_{0.98}In_{0.02}Sb$ was then freshly etched with CP4 etchant ($CH_3COOH:HF:HNO_3$ in 3:3:5 by volume). A seed of 20 mm in diameter, a $\langle 1\,1\,1\rangle$B oriented single crystal GaSb was used in the growth experiment. The melt was encapsulated by NaCl:KCl eutectic (50 mol%:50 mol%) alkali halide salt to avoid volatilization and to reduce the probability of multiple nucleation from the crucible wall. A pre-growth baking of the charge and the salt (to remove moisture) was carried out at approximately 300°C for a period of 3 h under vacuum. After the baking, the furnace was filled with 1 atm of argon and heated to about 10°C above the melting temperature of GaSb (712°C). The charge was homogenized by vertically raising and lowering the baffle in the melt for a period of 30–40 min. Thereafter, seeding was done by re-melting around 5 mm length of the seed. The melt was kept at a constant temperature for stabilization during 1 h. At the end of the homogenization cycle, the baffle was placed 1 cm away from the solid–liquid interface and the ampoule was lowered at a constant rate of 3.2 mm/h. The furnace temperature gradient near the melt–solid interface ($\mathrm{d}T/\mathrm{d}z$) was approximately 15 K/cm. This temperature gradient was sufficient to prevent constitutional super-cooling in $Ga_{0.98}In_{0.02}Sb$. After solidification, the furnace was cooled down slowly to room temperature, over a period of 8 h.

The experiments with Ga-doped Ge were also performed in 20 mm diameter silica crucibles, with a 20 mm diameter $\langle 1\,0\,0\rangle$ oriented Ge seed. No melt encapsulation was used in these experiments. The lowering rates were 10 and 30 mm/h. The distance h between the baffle and the melt–solid interface in two experiments was 1 and 1.5 cm. The third experiment started with $h = 1$ cm. During the growth, h continuously decreased as was evident from the temperature of the thermocouple in the baffle. No attempt was made to prevent the change in h. In the last to freeze section of the crystal, the baffle touched the melt–solid interface. This happened because the temperature of the hot zone was set too low, and therefore the growth interface was too close to the hot zone. In the earlier two experiments, the hot and cold zone temperatures were such that the melt–solid interface was near the center of the gradient. After solidification, the furnace was cooled down slowly to room temperature, over a period of 14 h.

The 20 mm seeds used in the above experiments (with GaSb and Ge) were grown from 5 mm diameter seeds. A typical seed of 20 mm diameter Ge grown from 5 mm diameter initial seed is shown in Fig. 1a. Subsequently grown crystal with the 20 mm diameter seed is shown in Fig. 1b. Due to carefully

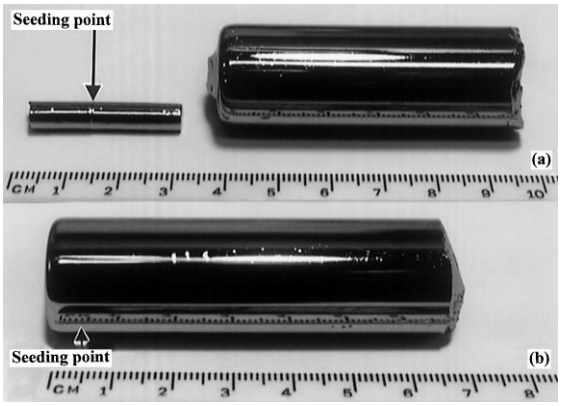

Fig. 1. (a) Single crystal of Ga-doped Ge, grown from 5 mm diameter seed, (b) single crystal of Ga-doped Ge, grown with a 20 mm diameter seed in a flat bottom crucible.

fitted seed, there was no leakage of the melt around the seed.

After growth, the ingots were sliced along the growth axis to evaluate the axial dopant profile. To evaluate the radial segregation profile, two slices were prepared along the growth axis from the center and edge of the crystal. The specimens were then lapped and mechanically polished with alumina powder with different grade to obtain mirror surface. The concentration of Ga in Ge was determined from measurements of the resistivity ρ, using a four point probe setup. The actual impurity concentration N (atoms/cm^3) was obtained using the following correlation [18]:

$$\rho = N^{-\alpha}/B, \tag{1}$$

where for p-type Ge (Ga-doped Ge), the values of α and B are indicated below in two different range of carrier concentrations:

$$B = 1.74 \times 10^{-11} \quad \text{and} \quad \alpha = 0.707$$

for $1 \times 10^{17} < N < 1 \times 10^{18}$,

$$B = 1.61 \times 10^{-10} \quad \text{and} \quad \alpha = 0.653$$

for $1 \times 10^{18} < N < 1 \times 10^{19}$.

The composition of the grown GaInSb crystal (Ga, In, Sb) was evaluated by electron probe micro-analysis (EPMA) measurements in a JEOL 733 electron microprobe set-up. The standards used were GaSb and InSb single crystal substrates. Corrections for atomic number (Z), self-absorption (A) and fluorescence (F) effects (ZAF corrections) were performed by employing the commercial software SCOTT-I. Composition error was in the order of 2–3% of the measured values. For example, if the measured composition of indium is 5 at%, the error in determination is $\sim$0.1 at%.

3. Results and discussion

Fig. 2 shows the axial and radial InSb concentration in the GaInSb crystal. There are three main regions: the initial transient, a steady-state region (where during diffusive controlled segregation, the dopant concentration should approach the initial melt concentration C_0) and the last to freeze region where the baffle is out of the melt. It is interesting to note that there is very little radial segregation in the crystal. Low radial segregation should be an indication of (i) flat solid–liquid interface and (ii) convective free segregation or perfect mixing. Perfect mixing clearly did not occur in the zone melt between the baffle and the interface. After the initial

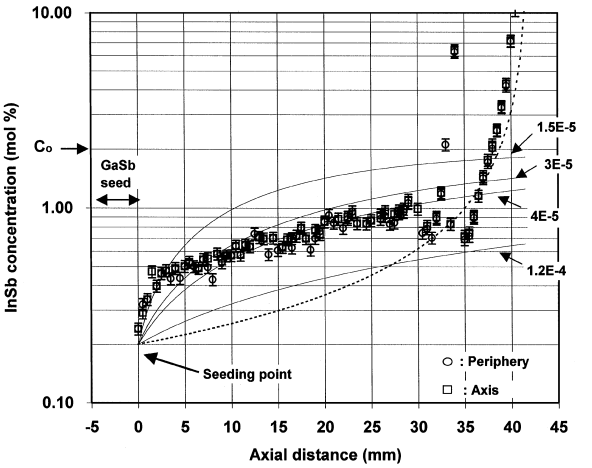

Fig. 2. Axial InSb concentration in GaInSb crystal ($C_0 = Ga_{0.98}In_{0.02}Sb$). Growth rate $R = 3.2$ mm/h. The open circles represent the InSb concentration along the central axis of the crystal; the open squares are obtained along the edge of the crystal. Solid lines are Tiller's equation with $k = 0.1$ and $D = 1.5$, 3.0, 4.0, 12×10^{-5} cm^2/s. Dashed line is the theoretically calculated profile for complete mixing using Pfann's equation [21].

transient, steady state typical for diffusion controlled growth was not reached in this experiment. The experimental data were fitted with Tiller's equation [19]:

$$\frac{C_s(x)}{C_0} = k + (1-k)[1 - e^{-(kR/D)x}], \quad (2)$$

where $C_s(x)$ is the dopant concentration in the solid at a distance x (cm) measured from the beginning of the specimen, D (cm^2/s) is the diffusion coefficient of the solute in the melt and R is the growth rate. The C_0 is equal to 2 mol% InSb : 98 mol% GaSb. The best fit of the Tiller's equation to the initial transient (see Fig. 2) gave $D_i = 1.5 \times 10^{-5}$ cm^2/s, where subscript "i" was used to designate the diffusivity of solute in the boundary layer at the interface, obtained during growth. D_i is eight times lower than the diffusivity reported in the literature (1.2×10^{-4} cm^2/s) measured in shear cells [15–17]. Based on D_i, the thickness of the solute layer can be estimated as

$$\delta \sim D_i/R = 0.164\,\text{cm}, \quad (3)$$

where it is assumed that the growth rate R is equal to the rate of lowering the crucible, $R = 0.33$ cm/h $= 9.17 \times 10^{-5}$ cm/s and $D_i = 1.5 \times 10^{-5}$ cm^2/s. Using the diffusivity reported in the literature, $D = 1.2 \times 10^{-4}$ cm^2/s yields

$$\delta \sim D_i/R = 1.31\,\text{cm}, \quad (4)$$

Consider that:

(i) Eqs. (3) and (4) present the thickness of the steady-state, "fully developed" solute layer, which should form after the initial transient, when the exponential term in Eq. (2) approaches zero.

(ii) At the very beginning of growth, the thickness of the solute layer is $\delta = 0$. The length of this initial transient is $x \sim 4$ cm (for $D_i = 1.5 \times 10^{-5}$ cm^2/s) or $x \sim 300$ cm (for $D = 1.2 \times 10^{-4}$ cm^2/s).

Based on (i) and (ii), we have to conclude that the solute layer could not have reached the baffle during the first 0.4 cm of growth (even if we used the high value of D reported in the literature, $D = 1.2 \times 10^{-4}$ cm^2/s). Therefore, the baffle did not interfere with diffusion at least within $0 < x < 0.4$ cm. Eq. (2) should be applicable because the baffle did not obstruct the development of the solute layer.

The D_i obtained from fitting the initial transient (the first 4 mm of growth) is close to the value in Te-doped GaSb [10]. This indicates that in the initial stages of growth, when the solute boundary layer contains low levels of In (~ 0.2 mol%), the diffusion is similar to that of an impurity in GaSb. As the boundary becomes rich in InSb, several factors may hinder the attainability of the perfect steady state. With the increase in InSb content in the solute boundary layer, the growth temperature decreases causing (a) reduction in growth rate R and thus, (b) increase in the zone height h. It can be seen from Eq. (2) that reduction in R has the same effect on $C_S(x)$ as increase in D: it will extend the initial transient in InSb concentration. The increase in zone height should increase the value of the Grashof number of the zone melt under the baffle, resulting in stronger convection which could alter the solute boundary layer (causing an increase in "effective diffusivity"). Since we did not use current pulsing for interface demarcation, and thus do not know the actual solidification rate, we fitted the second portion of the axial profile (10–30 mm) by assuming, as before, $R = 3.2$ mm/h. The best fit was obtained when fitted with $D_i = 3$–4×10^{-5} cm^2/s (corresponding to $\delta \sim D_i/R = 0.3$–0.4 cm). As evident from the figure, the value measured in shear cells [15–17], $D = 1.2 \times 10^{-4}$ cm^2/s, which is 3 to 4 times higher, is inadequate in fitting our experimental data (any section of the axial profile).

Fig. 3a shows the axial and radial Ga content in the Ge single crystal grown with 10 mm/h with a zone height of 10 mm. The initial transient (the first 8 mm of growth) could be fitted with a D_i of 8×10^{-5} cm^2/s which is much lower than what is reported in the literature from shear cell measurements [14] (2.1×10^{-4} cm^2/s). As in the GaInSb experiment, after the initial transient, the axial dopant composition exhibited a weak rise towards C_0 (7×10^{18} cm^{-3}). In the next experiment, the zone height was increased to 15 mm and the growth rate increased to 30 mm/h (as in the space experiment [20]) to reduce the length of the initial

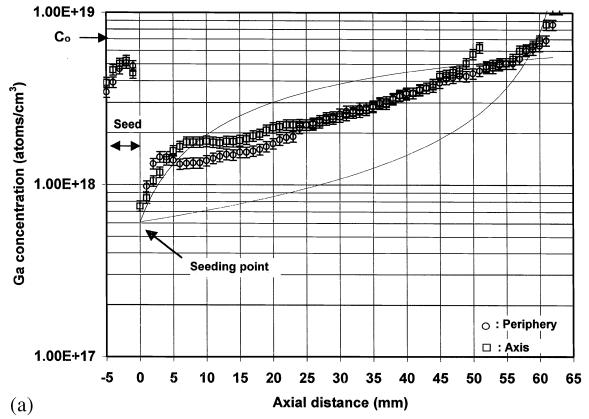

(a)

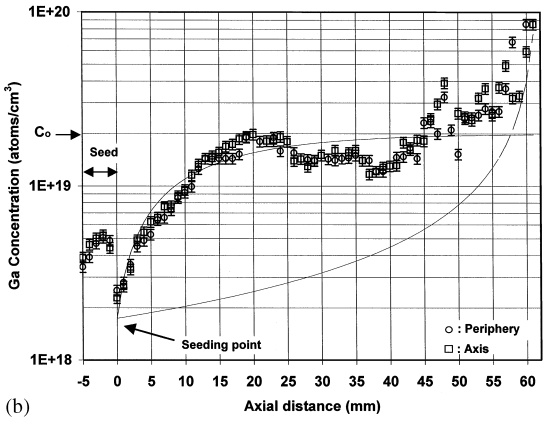

(b)

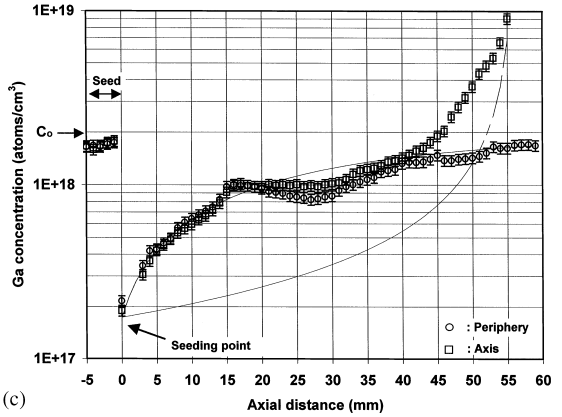

(c)

Fig. 3. Axial Ga concentration in Ge crystals: (a) $C_0 = 7 \times 10^{18}\,\mathrm{cm}^{-3}$, growth rate $R = 10\,\mathrm{mm/h}$; (b) $C_0 = 2 \times 10^{19}\,\mathrm{cm}^{-3}$, $R = 30\,\mathrm{mm/h}$; (c) $C_0 = 2 \times 10^{18}\,\mathrm{cm}^{-3}$, $R = 10\,\mathrm{mm/h}$. The open circles represent the Ga concentration along the central axis of the crystal; the open squares are obtained along the edge of the crystal. Solid lines are Tiller's equation with $k = 0.087$ and $D = 8.0 \times 10^{-5}\,\mathrm{cm}^2/\mathrm{s}$. Dashed line is the theoretically calculated profile for complete mixing using Pfann's equation [21].

transient and make segregation less sensitive to convection [11,12]. As a result, Ga concentration reached C_0 after about 25 mm of growth, Fig. 3b. The initial transient could be fitted well with $D_i = 8 \times 10^{-5}\,\mathrm{cm}^2/\mathrm{s}$. After the initial transient, Ga concentration exhibited a minima which can also be found in the space-grown crystal.

In the third experiment, the growth rate was kept at 10 mm/h, while the zone height continuously decreased from 10 to 0 mm during the growth. Once again, first 15 mm of the transient could be fitted with $D_i = 8 \times 10^{-5}\,\mathrm{cm}^2/\mathrm{s}$. The last to freeze portion of this crystal showed a large radial segregation because of diminishing zone height. This experiment demonstrates the effect of zone height on the axial and radial dopant distribution as a result of the modification in the shape of the solute boundary layer.

It is important to note that growth experiments in the presence of magnetic fields [3,4] and microgravity also yielded D lower than the shear cells [20], Table 1. The lack of steady state (such as reported in the experiment with Te-doped GaSb with $k = 0.37$) makes the values obtained from initial transients questionable. However, it is expected that the planed experiments with the submerged baffle in microgravity will provide the actual value of the diffusion coefficients.

Table 1
Diffusion coefficients D for Ga-doped Ge measured in the shear cells [14–17] and by fitting the initial transient of Ga concentration in crystals grown under axial magnetic fields [3,4], with submerged baffle (present work) and in space [20]

D (cm^2/s)	D_i (cm^2/s)	Method/comment	Reference
(a) System: InSb–GaSb			
	1.5×10^{-5}	Growth with submerged baffle/first 4 mm of growth	Present work
	$3–4\times10^{-5}$	Growth with submerged baffle/10–30 mm of growth	Present work
1.2×10^{-4}		Shear cell	[15–17]
(b) System: Ga-doped Ge			
	0.8×10^{-4}	Growth with submerged baffle	Present work
	1.25×10^{-4}	Bridgman growth/5 T	Szofran [4]
	1.5×10^{-4}	Bridgman growth/3 T	Matthiesen et al. [3]
	1.9×10^{-4}	Bridgman growth/in space	Witt et al. [2]
2.1×10^{-4}		Shear cell	Bourret et al. [14]

4. Summary

Solute segregation in two model materials: Ga-doped Ge and dilute alloy of GaInSb having low segregation coefficients was investigated using the submerged heater method. The values of diffusion coefficients extracted from the initial transients of axial dopant profiles ($D_i = 0.8\times10^{-4}$ cm^2/s for Ga-doped Ge and $D_i = 1.5\times10^{-5}$ cm^2/s for dilute GaInSb) are significantly lower than what is reported in the literature from shear cell measurements.

Acknowledgements

This work is supported by the Microgravity Science and Applications Division of the National Aeronautics and Space Administration.

References

[1] G. Müller, Convection and inhomogeneities in crystal growth from the melt, Crystals: Growth, Properties and Applications,Vol. 12, Springer, Berlin, 1988.
[2] A.F. Witt, H.C. Gatos, M. Lichtensteiger, M.C. Lavine, C.J. Hermn, J. Electrochem. Soc. 122 (1975) 276.
[3] D.H. Matthiesen, M.J. Wargo, S. Motakef, D.J. Carlson, J.S. Nakos, A.F. Witt, J. Crystal Growth 85 (1987) 557.
[4] F. Szofran, Personal Communication, 1996–1998.
[5] J. Kang, Y. Okano, K. Hoshikawa, T. Fukuda, J. Crystal Growth 140 (1994) 435.
[6] A.G. Ostrogorsky, G. Müller, J. Crystal Growth 137 (1994) 64.
[7] A.G. Ostrogorsky, J. Crystal Growth 104 (1990) 233.
[8] A.G. Ostrogorsky, F. Mosel, M.T. Schmidt, J. Crystal Growth 110 (1991) 950.
[9] A.G. Ostrogorsky, H.J. Sell, S. Scharl, G. Müller, J. Crystal Growth 128 (1993) 201.
[10] P.S. Dutta, A.G. Ostrogorsky, J. Crystal Growth 197 (1999) 749.
[11] A.G. Ostrogorsky, G. Müller, J. Crystal Growth 128 (1993) 207.
[12] A.G. Ostrogorsky, Z. Dragojlovic, Proceedings of the International Aerospace Congress, Moscow, Russia, 1994.
[13] P.S. Dutta, A.G. Ostrogorsky, J. Crystal Growth 191 (1998) 904.
[14] E. Bourret, J.J. Favier, O. Bourrel, J. Electrochem. Soc. 128 (1981) 2437.
[15] C. Raffy, T. Duffar, Internal Report, CEA-Grenoble, France, SES No. 15/95, 1995.
[16] T. Duffar, personal comunication.
[17] G. Müller-Vogt, ESA Report.
[18] S.M. Sze, J.C. Irvin, Solid State Electron. 11 (1968) 599.
[19] W.A. Tiller, K.A. Jackson, J.W. Rutter, B. Chalmers, Acta Metall. 1 (1953) 428.
[20] A.F. Witt, H.C. Gatos, M. Lichtensteiger, C.J. Hermn, J. Electrochem. Soc. 125 (1978) 1832.
[21] W.G. Pfann, J. Metals 194 (1952) 747.